ELSEVIER

Thin-Walled Structures 37 (2000) 147–162

THIN-WALLED STRUCTURES

www.elsevier.com/locate/tws

Dynamic analysis of piezoceramic actuation effects on plate vibrations

B. Proulx, L. Cheng *

Department of Mechanical Engineering, Laval University, Laboratory of Vibro-A, Québec, G1K 7P4, Canada

Received 9 July 1999; received in revised form 21 February 2000; accepted 1 March 2000

Abstract

This paper presents a simulation model for the active vibration control of a rectangular plate using piezoceramic elements of arbitrary shape. Experiments using multiple PZT patches were carried out to validate the model. An analysis was then undertaken to determine the dynamic effect of the piezoactuators. Numerical results showed that piezoactuators enhance the modal coupling of the structure under certain circumstances. Special attention should be paid to higher-order modes in both simulation and the development of active control strategies. Actuators of different shapes have been tested to show their influence on the dynamic behaviour of the structure. It was noted that actuators shapes affect the structure more in off-resonance regions than near resonance. This effect however remains weak as long as the actuators possess the same area and do not possess significantly different width to length dimensions.

Keywords: Vibrations; Plate; Active control; Piezoceramic; Sensor; Actuator; Simulation; Experiment

1. Introduction

Active vibration control using piezoceramic elements has attracted the attention of many researchers over the past decade. Due to the reversible effects of such materials when polarized, they can be used both as sensors and actuators in active vibration and noise control applications. In order to achieve optimal control perform-

* Corresponding author. Tel.: +1-418-656-7920; fax: +1-418-656-7415.
E-mail address: li.cheng@gmc.ulaval.ca (L. Cheng).

0263-8231/00/$ - see front matter
PII: S0263-8231(00)00013-6

ance, it is essential to have a full understanding of the actuation effects generated using piezoceramic actuators.

Following the pioneering work of Crawley and de Luis [1], efforts have been made during the last few years to develop suitable simulation models facilitating such analyses. Simple structures such as flexural beams and plates have been extensively investigated. A considerable number of papers have been published to establish various static models neglecting the dynamic effects of the piezo-elements [2–7]. It is generally assumed in these static models that the piezoelectric elements do not significantly affect the inertia mass and stiffness of the host structures. However, situations may occur where mechanical coupling between the piezo-elements and the host structures becomes strong, especially when a large number of sensors and actuators are needed to perform MIMO control. In this case, as pointed out by Chaudhry and Rogers [8], a simulation model capable of taking the full coupling into account is necessary for the accurate prediction of the frequency response of the structure. Recent works developing dynamic models using beam models have been reviewed in a recent paper by Brennan et al. [9]. Results reported both in that paper and other investigations [10] clearly show the necessity of such dynamic models. However, as regards two-dimensional structures, much less work has been done. Two-dimensional structures involve more significant coupling in different coordinate directions. Dynamic coupling between the host structure and piezo-elements is also reinforced. It is therefore highly desirable to develop appropriate dynamic models for such structures as claimed by Zhou et al. [11], who proposed an impedance-based approach. By applying the latter to both shell and plate structures, it was shown that the dynamic performance of the host structure and the actuators could strongly influence each other.

In the present paper, a dynamic model is presented to analyse the actuation effects of the piezo-elements on vibrations of a plate with symmetrically placed piezo-elements. Using this model, actuators of arbitrary shapes can be modelled. Vibration sensing using shaped piezoelectric sensors has been investigated by many researchers in the past. However, the effects of shaped actuators have attracted much less attention up to now. Active control using shaped actuators may present special interests in certain applications. This issue has been addressed by Sonti et al. [12]. Using specific configurations, they performed a static analysis to obtain the equivalent forces and moments of actuators of different elementary shapes. It was noted that in addition to the line moment, transverse forces may also exist varying with the contour shape of the actuators. The effects on the structure in terms of dynamic response however still remain to be investigated. The present analysis can be used to deepen our understanding of the issue.

The additive property is shown to hold for both actuators and sensors. A whole PZT element can then be discretized into small rectangular pieces. A dynamic model using a rectangular plate with symmetrically placed rectangular piezo-elements have been independently developed in our past work [13] and by Charette et al. [14]. The model was based on a variational approach using springs at the boundary and a polynomial decomposition for the transverse displacements. In the present paper, this model will be extended to the actuators of arbitrary shape based on the aforementioned principle. Experimental validations were performed using multiple PZT

patches. Compared to results reported previously, piezoceramic sensors were also considered. The lack of experimental data in the literature is a deplorable fact. Experimental results presented in the present give useful information in this regard. Coupling analysis was then carried out for a typical configuration to show the effect of the actuators. The influence of the actuator shape (rectangular, circular, oval etc.) was then investigated.

2. Modeling procedure

The basic system consists of a thin rectangular plate (dimensions 2b, 2h, 2e), on which PZT patches of arbitrary shape are bonded on each side as illustrated in Fig. 1. The piezoceramic elements serve either as sensors or actuators and are assumed to be perfectly bonded to the plate. The boundary conditions of the plate are simulated by introducing a set of uniformly distributed virtual springs along each edge. A proper combination of the spring stiffness makes it possible to simulate all classical boundary conditions. Since part of the development is similar to the one used previously [13,14], it is therefore presented in a brief way.

A piezo-element such as the one illustrated in Fig. 1 is first discretized into a number of small rectangular cells. It was shown that if proper deformation (such as the one defined by Kirchhoff–Love assumptions) is imposed on each cell, the additive property is shown to hold [13]: the effect of the whole actuator (or sensor) will be the superposition of the all rectangular cells if the mesh is properly defined. In fact, the use of Kirchhoff–Love assumptions ensures the continuity between each pair of adjacent cells so that the total effect will be the same as a single piece. In doing so, modelling can be done for each rectangular element and the same criteria used in the finite element analysis can be used to determine the number of mesh that should be used.

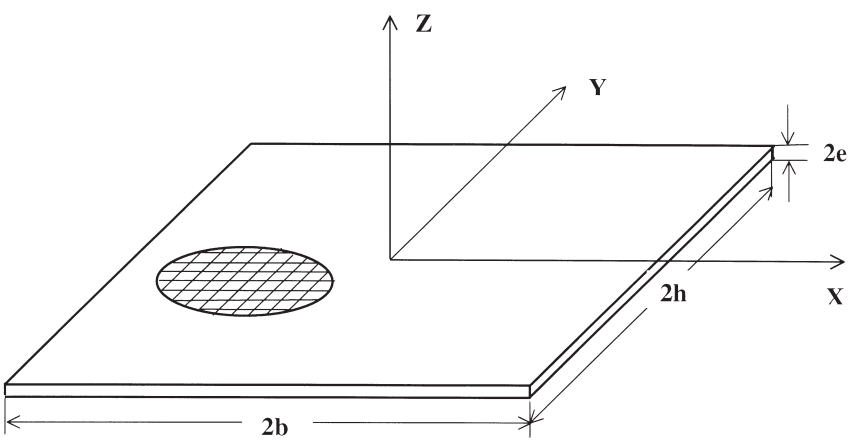

Fig. 1. Schematic representation of a rectangular plate with integrated piezoceramic elements.

Kirchhoff–Love assumptions are used to build the displacement field for the plate and each PZT cell as follows:

$$\{u,v,w\}=\left\{-z\frac{\partial w}{\partial x},-z\frac{\partial w}{\partial y},w(x,y,t)\right\} \tag{1}$$

where the vector $\{u, v, w\}$ represents the displacement of a point either on the plate or on the piezoceramic elements. Perfect bonding is considered between the plate and the piezoelectric pieces, leading to a continuity of extensional displacements at all interfaces.

Rayleigh–Ritz approximations are used to solve the system with the following polynomial series expansion in terms of x and y:

$$w(x,y,t)=\sum_{i=0}^{m}\sum_{j=0}^{n}a_{ij}(t)\left(\frac{x}{b}\right)^i\left(\frac{y}{h}\right)^j \tag{2}$$

where $a_{ij}(t)$ are the complex and time-dependent variables to be determined.

The analytical formulation is based on the variational approach, in which the energy of the whole system is extremalized by means of the Lagrange equations. Using the coefficients $a_{ij}(t)$ as the generalized coordinates, Lagrange equations can be written in the general form:

$$\frac{\mathrm{d}}{\mathrm{d}t}\left(\frac{\partial L}{\partial \dot{a}_{pq}}\right)-\frac{\partial L}{\partial a_{pq}}=0 \quad (p=0,1,2,...,m \text{ and } q=0,1,2,...,n) \tag{3}$$

where L is the Lagrangian of the system expressed as:

$$L=E_\mathrm{k}-E_\mathrm{p}+W \tag{4}$$

where E_k represents the total kinetic energy of the system, E_p the total potential energy of the system and W the work done by the external forces.

With the assumption of thin plates and symmetric installation of the PZT elements, the kinetic energy of each element (plate, actuators and sensors) is represented as:

$$E_\mathrm{k}=\frac{1}{2}\int_v \rho\left(\frac{\partial w}{\partial t}\right)^2 \mathrm{d}V \tag{5}$$

where V represents the volume, ρ the density and w the flexural displacement for each element. The potential energy of the plate is obtained from the integral of the stress multiplied by the strain over the complete volume:

$$E_\mathrm{p}^{\mathrm{plate}}=\frac{1}{2}\int_v (T_{11}S_{11}+2T_{12}S_{12}+T_{22}S_{22})\mathrm{d}V \tag{6}$$

The stress terms T_{ij} and the strain terms S_{ij} can be easily expressed in terms of the displacement of the plate using Eq. (1). Boundary conditions are represented by a set of virtual rotational and translational springs equally distributed along each edge of the plate (K_i in N/m^2 for translation and C_i in N/rad for rotation, i=1, 2, 3, 4).

The whole procedure yields the following expression for the potential energy of the plate with elastic boundaries:

$$E_{\mathrm{p}}^{\mathrm{plate+boundary}}=\int_V \frac{Yz^2}{2(1+v)}\left\{\frac{1}{(1-v)}\left[\left(\frac{\partial^2 w}{\partial x^2}\right)^2+\left(\frac{\partial^2 w}{\partial y^2}\right)^2+2v\frac{\partial^2 w}{\partial x^2}\frac{\partial^2 w}{\partial y^2}\right]+2\left(\frac{\partial^2 w}{\partial x\partial y}\right)^2\right\}\mathrm{d}V+$$

$$\frac{1}{2}\int_{-h}^{h}\left\{k_1[w(-b,y,t)]^2+k_2[w(b,y,t)]^2+c_1\left[\frac{\partial w(-b,y,t)}{\partial x}\right]^2+c_2\left[\frac{\partial w(b,y,t)}{\partial x}\right]^2\right\}\mathrm{d}y+$$

$$\frac{1}{2}\int_{-b}^{b}\left\{k_3[w(x,-h,t)]^2+k_4[w(x,h,t)]^2+c_3\left[\frac{\partial w(x,-h,t)}{\partial y}\right]^2+c_4\left[\frac{\partial w(x,h,t)}{\partial y}\right]^2\right\}\mathrm{d}x \quad (7)$$

where Y, and v are respectively the complex Young's Modulus and the Poisson coefficient of the plate. The work done by an external point force excitation is given by:

$$W_\delta=f_\delta(t).w(x_\delta,y_\delta,t) \quad (8)$$

where f_δ is the external point force applied to the plate and $(x_\delta y_\delta)$ the application point.

The total enthalpy density of a piezoelectric element [15] is used to find the potential energy of the piezoceramic elements by considering only the transverse electric field E_3

$$H=0.5[T_{11}S_{11}+T_{22}S_{22}+2T_{12}S_{12}]-[\mathrm{e}_{31}E_3(S_{11}+S_{22})]-[0.5\varepsilon_{33}E_3^2] \quad (9)$$

where H is the enthalpy density; ε_{33} the permitivity; T_{ij} the stress; S_{ij} the strain and e_{31} the piezoelectric constant.

After minimization using Eq. (9), for actuators, the first term represents the rigidity of the piezoelectric elements, the second, the energy supplied by the actuator to the structure, and the last term disappears. Eq. (9) also applies to the sensors. Being passive elements however, only the first term of Eq. (9) is retained representing their rigidities.

In addition, the impedance of the circuit connected to the sensor modifies its Young's modulus. In the case of an open electrode configuration, the impedance goes to infinity so that the Young's modulus would be higher than that of the closed electrode circuit. This is the case when a PZT is not connected to an electric circuit. The relation between the open and closed electrode Young's modulus of piezoelectric sensors is as follows:

$$\bar{Y}_{11}=Y_{11}/(1-d_{31}g_{31}Y_{11}) \quad (10)$$

where, $\bar{Y}_{11}$, is the open electrode Young's modulus, Y_{11}, the closed electrode Young's modulus, d_{31}, the strain/charge coefficients and g_{31}, the charge/stress coefficients.

The total potential energy of the whole system is given by:

$$E_p = E_p^{\text{plate+boundary}} + \int_{v_p} H \, dv \tag{11}$$

where v_p represents the volume occupied by piezo-elements. The last term of Eq. (11) applies to both sensors and actuators. As far as the sensors are concerned, one obtains the same expression as the first term of Eq. (7), related to their stiffness via the potential energy of the sensors. Care should be taken in replacing all the terms related to material properties by these of the sensors. In the case of the actuators, one obtains:

$$\int_{v_p} H dv = \int_{v_p} \frac{Y_{11}^{\text{piezo}} z^2}{2(1+\nu_p)} \left\{ \frac{1}{(1-\nu_p)} \left[\left(\frac{\partial^2 w}{\partial x^2} \right)^2 + \left(\frac{\partial^2 w}{\partial y^2} \right)^2 + 2\nu_p \frac{\partial^2 w}{\partial x^2} \frac{\partial^2 w}{\partial y^2} \right] + 2 \left(\frac{\partial^2 w}{\partial x \partial y} \right)^2 \right\} dv +$$

$$\int_{v_p} e_{31} \frac{\Delta\varphi}{e_p} z \left(\frac{\partial^2 w}{\partial x^2} + \frac{\partial^2 w}{\partial y^2} \right) - \frac{1}{2} \varepsilon_{33} \left(\frac{\Delta\varphi}{e_p} \right)^2 dv \tag{12}$$

where $\Delta\varphi$ stands for the voltage applied to the actuators and e_p is the thickness.

Using the Lagrange Eq. (3) with Eq. (2) leads to the following differential equations of the system:

$$[\mathbf{M}]\ddot{\mathbf{A}}(t) + [\mathbf{K}]\mathbf{A}(t) = \{\mathbf{F}(t)\} + \{\mathbf{Q}(t)\} \tag{13}$$

where [**M**] and [**K**] are, respectively, the mass matrix and the stiffness matrix. **F**(t) is the external force vector and **Q**(t) the excitation provided by the actuators.

Using Eq. (13), both the free and the forced vibrations of the structure can be treated. In the case of forced vibrations, Eq. (13) is resolved using harmonic excitations. In addition, a damping factor is introduced in the Young's modulus of the plate to represent the damping of the system. The accuracy of the results depends mainly on the truncation of the series used in Eq. (2). This issue have been discussed in detail in a previous publication [16]. For the free vibration analysis, the natural frequencies and the corresponding mode shapes can be found by resolving the eigenproblem of Eq. (13).

The electric charge of the sensor is obtained from the electric field derived from the enthalpy density H. For closed circuit sensors, one can express the dielectric displacement D_3 (charge per unit area) by:

$$D_3 = \varepsilon_{33} E_{33} + d_{31} T_1 + d_{32} T_2 + d_{36} T_6 \tag{14}$$

where ε_{33} is the permitivity constant and d_{ij} the piezoelectric constants.

The electrical charge $q(t)$ can be found by integrating the electric displacement over the surface of the electrode:

$$q(t) = \int D_3 \, dx dy \tag{15}$$

Using the capacitance C, the output voltage of each sensor is given by:

$$V_s = -\sum_{p=0}^{m}\sum_{q=0}^{n}\frac{1}{2C}(e_s+2e)a_{pq}(t)\left\{\left[e_{31}\frac{px^{p-1}}{b^p}\frac{y^{q+1}}{(q+1)h^q}\right]+\left[e_{32}\frac{qy^{q-1}}{h^q}\frac{x^{p+1}}{(p+1)b^p}\right]\right\} \quad (16)$$

where e_s is the thickness of the PZT sensors.

3. Experimental validations

Experimental tests were performed to validate the proposed models using rectangular PZT elements. Fig. 2 shows the experimental set-up and associated equipment. To create free boundary conditions, the plate was suspended from a stiff steel frame by two rubber bands of very weak stiffness attached to the middle of two opposite sides of the plate. Actuator patches were used to excite the structure.

Polytec PIC 141 piezoceramic patches were used for the tests. Six pairs of piezo-elements were bonded to the plate surface at locations illustrated in Fig. 3. Characteristics of the plate and the piezo-elements are summarized in Table 1. Before bonding the piezoelectric elements, the plate was anodized to isolate the plate from the piezoelectric pieces. For each piezoceramic element, a groove was machined into the plate for positioning and welding the conductors. Efforts were made to develop a good welding procedure. Small grooves in the plate helped avoid the plate and the piezoelectric element from shearing loose and the matching of the simulation results and

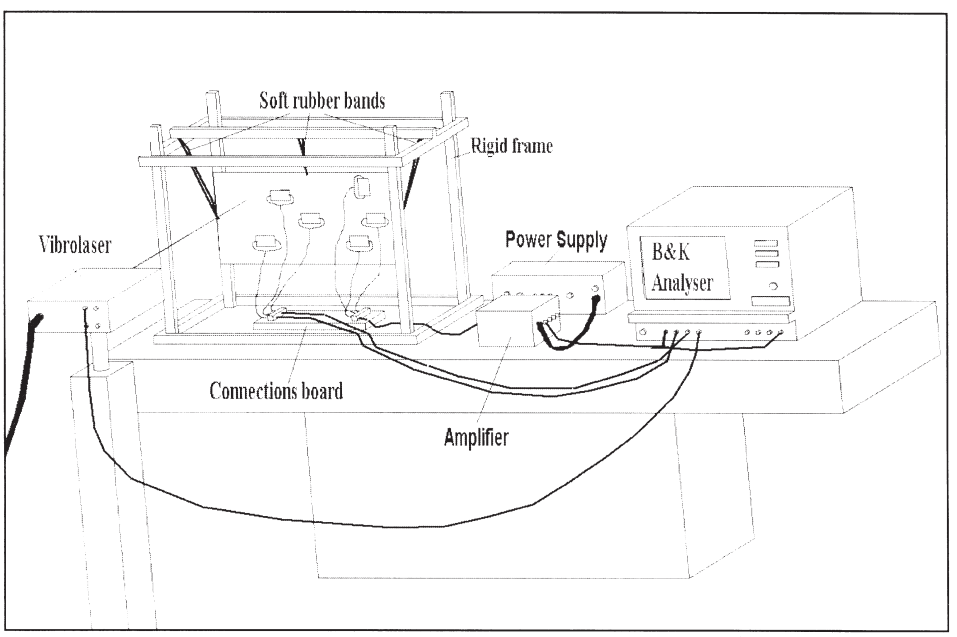

Fig. 2. Experimental set-up.

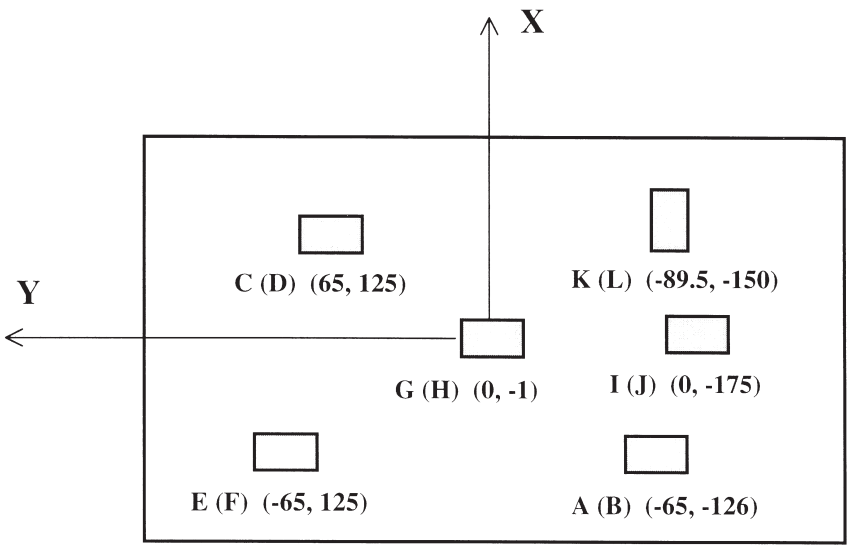

Fig. 3. Locations of PZTs.

Table 1
Dimensions and physical properties of the system

	Plate	PZT elements
Width (2*b*) [m]	0.260	0.03
Length (2*h*) [m]	0.500	0.05
Thickness (2*e*)[m]	0.226 E-2	0.4 E-3
Density (ρ)[kg/m^3]	2700	7800
Permitivity	–	0.1157 E-7
Young's modulus (*E*) [Pa]	7E+10	0.79365E11
Piezoelectric constant (e_{31})	–	9.127 [N/m.V]
Loss factor	0.01	–
Poisson ratio(ν)	0.30	0.30

the experimental data. In addition, the welding temperature must be kept lower than the Curie temperature to avoid depolarization. Copper wires of 0.1 mm in diameter were used as conductors. With the latter and a suitable welding technique, the size of the welding spots could be kept within 1.5 mm long, 1 mm wide and 0.2 mm thick. Groove dimensions have been chosen to be 3.175 mm long, 1.588 mm wide and 0.254 mm thick. These dimensions allow us to minimize as much as possible the discrepancies between the model and the experimental set-up. Loctite Superbonder 496 was used to glue the piezo-elements to the plate, with an adhesive layer about 0.04 mm thick.

A white noise (0–800 Hz) generated by the 2035 B&K analyser was amplified

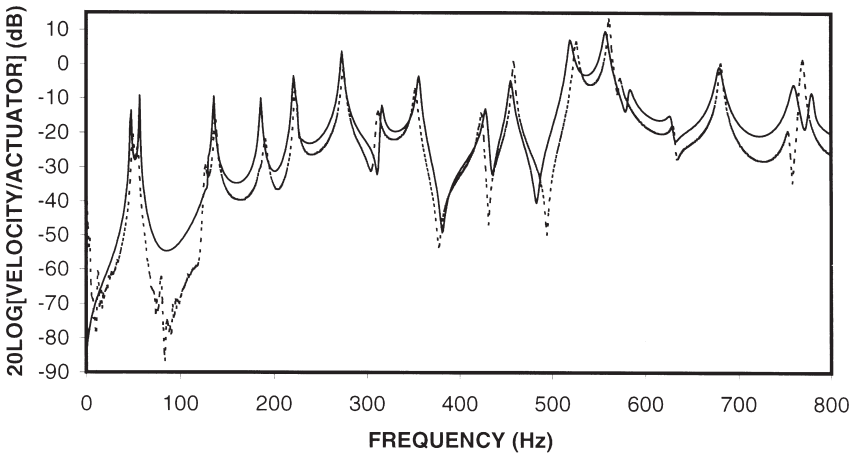

Fig. 4. Comparison between simulation and experiment in terms of velocity/actuator transfer function: Actuators A(B). Simulation: ———; Experiment: - - -.

by a power amplifier and then applied to a selected pair of PZTs. A single piezo-element or a laser vibrometer was used to measure the plate response. Comparisons between simulation and experimental transfer functions are compared using three different configurations. In simulations, all spring stiffness parameters of the boundary are set to be zero. In all cases, the PZT pair A(B) is used as actuator.

First of all, the velocity/actuator transfer functions were compared. The laser vibrometer measured the velocity of the plate at point (50, 170 mm). The transfer function presented in dB (referenced to 1) is shown in Fig. 4. Sensor output was then investigated. Fig. 5 compares the sensor/actuator transfer function between actu-

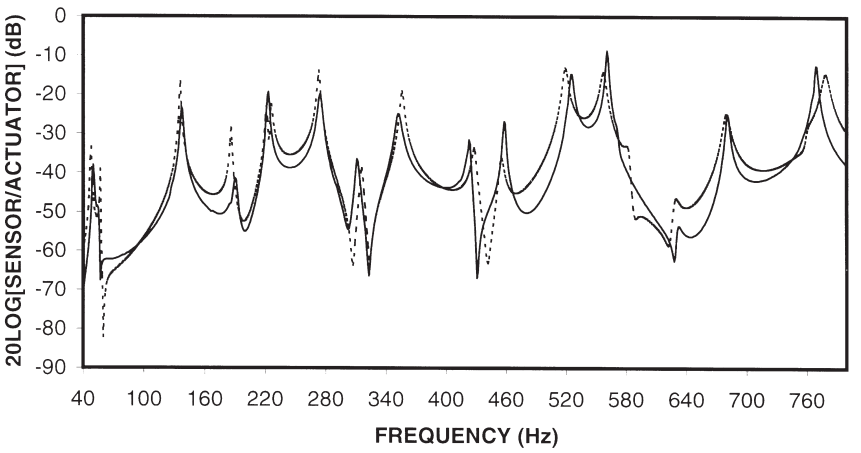

Fig. 5. Comparison between simulation and experiment in terms of sensor/actuator transfer function: Actuators A(B); sensor E(F). Simulation: ———; Experiment:- - -.

ators A and B and sensors **E**(**F**). Same comparisons were made in Fig. 6 using another sensor pair **I**(**J**). It can be seen that resonant peaks are well predicted by the simulation model, showing that both the boundary conditions of the plate and the mass and stiffness effects of the PZT are reasonably well simulated. At higher frequencies, numerical and experimental results demonstrate the same tendency. Generally speaking, it can be seen that good agreement is obtained in all cases. The model is particularly accurate in the low and middle frequency ranges as well as in resonance regions. More obvious discrepancies can be observed in off-resonance regions and this state of affairs is slightly amplified with the increase in frequency. This difference may be attributed to the exclusion of the bounding layer in the simulation model, which certainly becomes more important and necessary to take into account of at high frequencies. However the model seems to be accurate enough to predict the general dynamic tendency of the system for most active control simulation purposes. It should be mentioned that, compared to most of the comparisons presented in the literature, the present configuration covers a large number of modes, representing such a relatively more complex system. We conclude that the developed model is very representative of a physical system composed of a panel with multiple integrated piezo-elements.

4. Actuation effects

Numerical analyses were performed using the proposed model. In particular, special attention was first paid to analyzing the dynamic coupling effects. A typical analysis is presented to show the actuation effect of the PZT elements. The previous plate was again used for this analysis, except for the fact that the plate was clamped along all its edges and only PZTs A(B) and C(D) were bonded to the surface of the

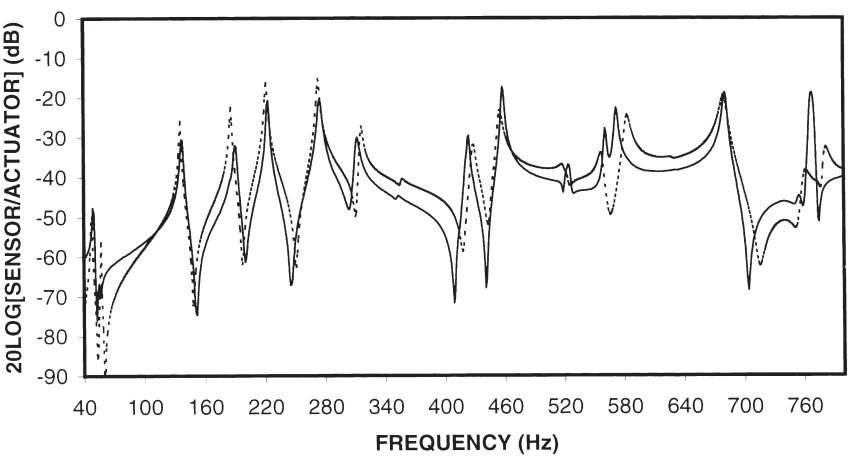

Fig. 6. Comparison between simulation and experiment in terms of sensor/actuator transfer function: Actuators A(B); sensor **I**(**J**). Simulation:———; Experiment: - - -.

plate. The stiffness parameters of the boundary springs are set to be higher enough than the flexural stiffness of the plate (10^8 times higher). Two excitations were considered. First, a force excitation located at (-40.5, -55 mm) was used to drive the plate with the acceleration response calculated at (-48, 54.5 mm). Second, PZTs A(B) was used as excitation. The acceleration/actuator transfer function curve is compared with the acceleration/force one in Fig. 7. It should be noted that a comparison of the absolute values of both curves is meaningless, since the piezo-actuator generates excitations distributed over the whole area whilst the force is a punctual excitation. However, a comparison of the overall tendency of the data reveals a particular behavior that is of practical importance. It can be seen that both excitations result in almost identical tendencies in terms of modal response except at the lowest frequencies. Before the first resonance frequency, the behavior of the plate with activated actuators is rather more complex than the force-excited one. In fact, the actuator-driven curve drops off significantly at 104 Hz before the first natural frequency of the plate (126 Hz). We noticed that this phenomenon usually happens when the plate has at least two opposed clamped boundaries. A similar phenomenon has also been observed experimentally using a clamped-free beam. Further analyses were carried out to understand this observation. To this end, the deformations of the plate were plotted at 104 Hz for both the force-driven and actuator-driven plate. The two corresponding surfaces are presented in Fig. 8(a,b) respectively. In order to visualize better the deformation, a cross section passing through the center of the actuators and parallel to the Y-axis is used. It can be seen from Fig. 8(a) that when the plate is excited by the force, the deformation takes the form of the first mode of the plate, since the analyzed frequency is lower than and close to the first natural frequency of the plate. When excited by the actuator however, the plate deformation is much more complex as illustrated in Fig. 8(b). This observation suggests that even before the first natural frequency of the 12 plate, not only the first mode is important,

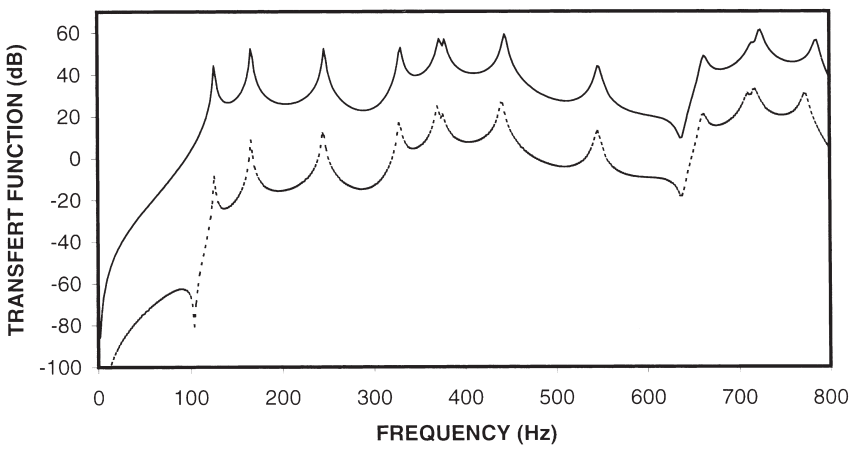

Fig. 7. Comparison between a force excitation and an actuator excitation in terms of transfer function. Force excitation: ———; PZT actuator: - - -.

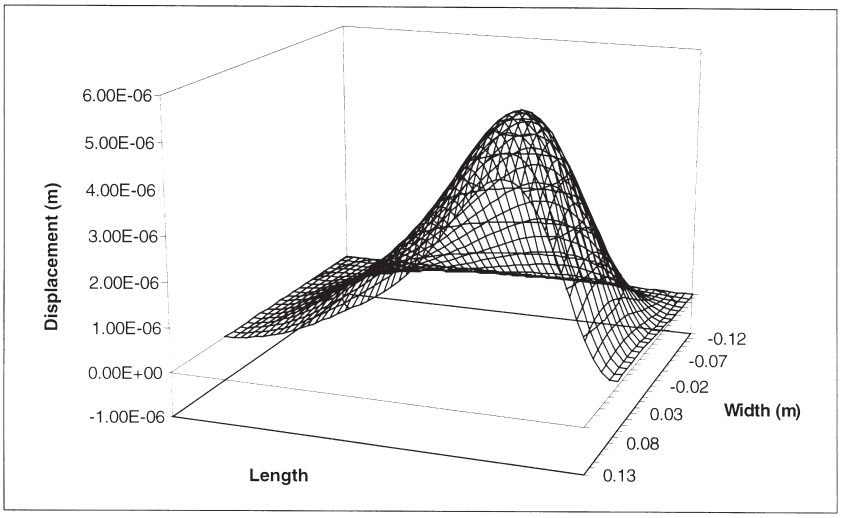

(a)

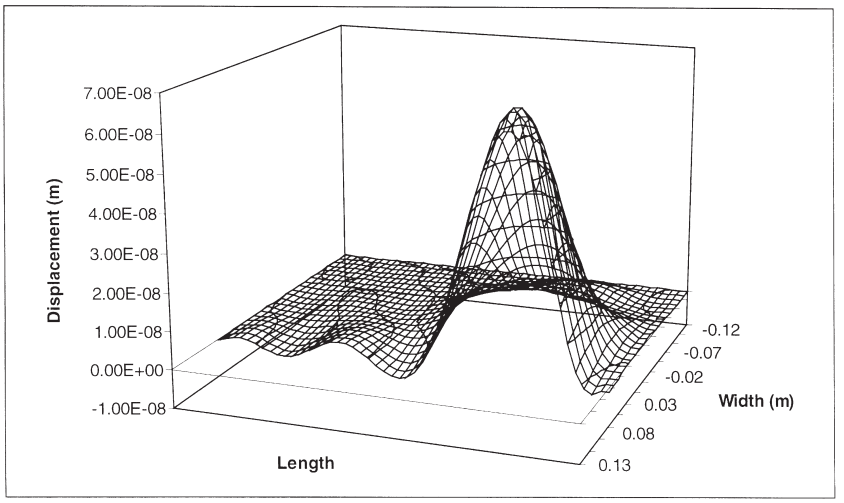

(b)

Fig. 8. Deformation of the plate at 104 Hz. (a): force excitation; (b): actuator excitation.

but also higher-order modes that significantly contribute to the response of the system, despite the fact that their natural frequencies are much higher than the excitation frequency. It is clear that using an actuator as excitation amplifies the modal coupling of the system. Two immediate consequences follow this observation. From the simul-

ation stand point, simulation of the system with actuators is more demanding than the one with force excitation, since more modes (using a modal approach) or terms (using the Rayleigh–Ritz approach) are necessary to achieve good accuracy. Another consequence is directly related to development of a control strategy based on the modal approach: care must be taken to control higher-order modes since they can significantly contribute to the response of the system even in a frequency zone far away from their natural frequencies.

The developed model was subsequently used to investigate the effects of the shapes of the actuators. Static effects of actuators of different shapes have been addressed by Sonti et al. [12]. The model presented previously can be used to investigate the dynamic effects of actuators in terms of dynamic response. To this end, the piezo-elements was first discretized into a number of small rectangular elements. The additive property can be shown to apply, permitting one to handle the actuator form as a combination of a series of smaller sized elements. The displacement field used in the model ensures the continuity between each adjacent element. In this way, the previously developed model can be used directly, leading to a general formulation applicable to plate structures with piezo-elements of any shape. Sufficient meshing of the actuator ensures a good approximation of the real shape. Using the configuration defined previously, Fig. 9 illustrates the convergence curve using different discretizations and the corresponding response curve when an oval actuator is used. The convergence parameter used in this figure is the integral of the quadratic velocity curve over a given frequency range (0–1200 Hz). It can be seen that convergence is achieved using a 400×400 mesh.

In order to illustrate the effect of the actuator shape on the response of the system, the previous configuration was used again. Using the same sensor as before, the transfer functions were calculated using four different actuators possessing the same surface area. The four actuators were a rectangle (the one used before), a circle and

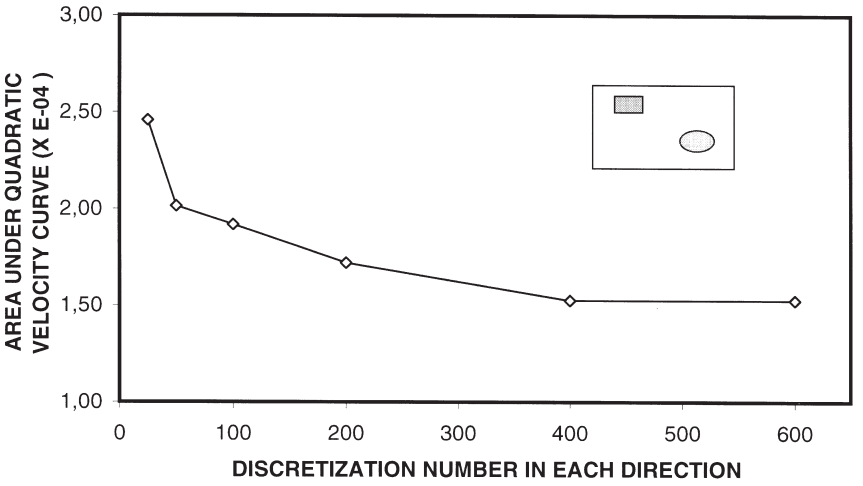

Fig. 9. Convergence curve using different discretizations with oval actuators.

two ellipses respectively with ratio of minor to major axes of 1:4 and 1:16. Several interesting points are worth mentioning. Comparing the data from the first three configurations illustrated in Fig. 10, it can be seen that by keeping the surface area constant, the actuator shape does not visibly affect the response curves at resonances. More obvious discrepancies only appear in the off-resonance regions. Note that all the first three configurations possess roughly comparable dimensional ratios (3:5 for the rectangle, 1:1 for the circle and 1:4 for the ellipse). The fourth curve illustrates the case of a highly flattened actuator (i.e. ratio 1:16). It can be seen that the influence of the actuator shape in this case becomes more apparent with the increase in frequency. This is understandable since this disproportionally shaped actuator covers a greater distance of the plate surface, which is very different than the first three cases. As a result, it strongly disturbs the modal response of the system with significant effects in the off-resonance regions. It can therefore be concluded that actuators of different shapes do not strongly disturb the response of the structure unless they are disproportionally shaped in their dimensions. The effects in this case are then much more apparent in the off-resonance regions.

5. Conclusions

Effects of PZT actuation have been investigated in the present paper. The principal findings can be summarized as follows:

1. Experimental validations are undertaken using a configuration involving relatively complex modal behaviour, resulting in satisfactory agreement. The simulation model seems to provide good accuracy when multiple patches of PZT are used.

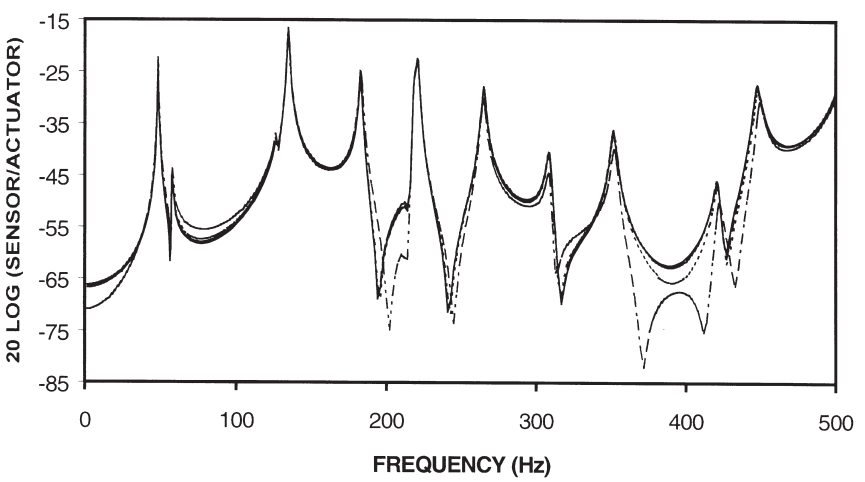

Fig. 10. Influence of the actuator shape on the response of the system. Rectangular: ———; Circle:- - -; Ellipse 1:4:· · ·; Ellipse 1:16:– · –.

2. Numerical results show that piezoactuators enhance the modal coupling of the structure under certain circumstances. Special attention should be paid to higher-order modes in both simulation and the development of active control strategies. The contribution of some modes may be strong even when their natural frequencies are far away from the excitation frequency.
3. Actuators of different shapes affect the structure more in off-resonance regions than near resonance. This effect however remains weak as long as the actuators possess the same area and do not possess significantly different width to length dimensions.

Acknowledgements

The authors gratefully acknowledge the support of the Structure R&D, de Havilland and NSREC, with B. Leigh and R. Lapointe as technical monitors. The technical assistance of Y. Jean, Y. St-Amant and M. Gignac during the experimental tests was also greatly appreciated.

References

[1] Crawley EF, de Luis J. Use of piezoelectric actuators as elements of intelligent structures. AIAA J 1987;259:1373–85.
[2] Dimitriadis EK, Fuller CR, Rogers CA. Piezoelectric actuators for distributed vibration excitation of thin plates. Trans ASME J Vib Acoust 1991;113:100–7.
[3] Lee CK, Chiang WW, O'Sullivan TC. Piezoelectric modal sensor/actuator pairs for critical active damping vibration control. J Acoust Soc Am 1991;90:374–84.
[4] Gibbs GP, Fuller CR. Excitation of thin beams using asymmetric piezoelectric actuators. J Acoust Soc Am 1992;96:3221–7.
[5] Kim SJ, Jones JD. Influence of piezo-actuator thickness on the active vibration control of a cantilever beam. J Int Mat Syst Struct 1995;6:2047–53.
[6] Koshigoe S, Mudock JW. A unified analysis of both active and passive damping for plates with piezoelectric transducers. J Acoust Soc Am 1993;93:346–55.
[7] Clark RL, Flemming MR, Fuller CR. Piezoelectric actuators for distributed vibration excitation of thin plates: a comparison between theory and experiment. Trans ASME, J Vib Acoust 1993;115:332–9.
[8] Chaudhry Z, Rogers CA. Performance and optimization of induced strain actuated structures under external loading. AIAA J 1994;32:1289–94.
[9] Brennan MJ, Elliott SJ, Pinnington RJ. The dynamic coupling between piezoceramic actuators and a beam. J Acoust Soc Am 1997;102:1931–42.
[10] Plantier G, Guigou C, Nicolas J, Piaud JB, Charette F. Variational analysis of a thin finite beam excitation with a single asymmetric piezoelectric actuator including bonding layer and effects. Acta Acoust 1995;3:135–51.
[11] Zhou S, Liang C, Rogers CA. An impedance-based system modeling approach for induced strain actuator-driven structures. Trans ASME J Vib Acoust 1996;118:323–31.
[12] Sonti VR, Kim SJ, Jones JD. Equivalent forces and wavenumber spectra of shaped piezoelectric actuators. J Sound Vib 1995;187:111–31.

[13] Proulx B. Développement d'un modèle de simulation sur le contrôle actif d'une plaque mince avec des céramiques piézoélectriques. Master Thesis, Laval University, Québec, Canada 1997.
[14] Charette F, Berry A, Guigou C. Dynamic effects of piezoelectric actuators on the vibrational response of a plate. J Int Mat Syst Struct 1997;8:513–24.
[15] Jaffe B, Cook W, Jaffe H. Piezoelectric ceramics. London: Academic Press, 1971.
[16] Cheng L, Lapointe R. Vibration attenuation of panel structures by optimally shaped viscoelastic coating with added weight considerations. Thin-walled Struct 1995;21:307–26.